International Journal of Mechanical and Production Engineering Research and Development (IJMPERD)
ISSN (P): 2249-6890; ISSN (E): 2249-8001
Vol. 7, Issue 6, Dec 2017, 679-686

EFFECT OF CHEVRON ON THE DECAY CHARACTERISTICS OF COMPRESSIBLE ROUND JET

S. SENTHIL VELAVAN[1] & K. VIJAYARAJA[2]

[1]*Research scholar, Sathyabama University, Chennai, India*

[2]*Professor, KCG College of Technology, Chennai, India*

ABSTRACT

In the present study, the flow fields generated by two jets with a chevron and a conventional circular nozzle exits are studied and compared. Three different nozzle configurations were considered one with no chevron and the other two has 4 and 8 chevrons each. Each configuration, has been studied with two different exit Mach numbers. Centerline velocity decay and turbulent kinetic energy were analyzed and discussed. It is found that the flow field strongly depends on the exit geometry.

KEYWORDS: Chevron Nozzle, Noise Suppression Techniques, Subsonic Jets & Jet Decay

Received: Oct 27, 2017; **Accepted:** Nov 18, 2017; **Published:** Dec 18, 2017; **Paper Id.:** IJMPERDDEC201776

Original Article

INTRODUCTION

Due to strict regulations and associated environmental problems Aircraft-generated noise is a major concern in the aviation industry. Aircraft engine jet noise is the major source of noise generation, especially during take-offs and landings. As a result of these various attempts were made by the researchers to develop new innovative technologies to reduce the jet noise. This attracts massive amount of investments in the field of aeroacoustics research over the past few decades.

In the last decades, a few practical passive flow control techniques for jet noise reduction were developed such as tabbed nozzles, pylon installations, deflector plates, castellated nozzles, multi-lobed mixers, microjets, water injection, contoured plugged nozzle, chevrons, etc. The above techniques were suitable for the application in the commercial aircraft gas turbine engines but, it also associated with thrust losses. It must be minimized in-order to make these configurations a success.

Turbulence statistics based acoustic models were essential to predict the jet noise. In-regard to that numerous studies were reported on jet turbulence in the past. Davies et al., (1963) experimentally derived the length and time scales from the space-time measurements of cold, low-speed jets. Bradshaw et. al., (1963) documented the spatial correlations for all six components of the correlation matrix with three-dimensional displacements. Bridges and Wernet (2010) used Particle Image Velocimetry (PIV) to develop a consensus dataset of flow quantities for a range of hot jet including uncertainty bands. They created a catalog of turbulent jet flows that can be compared with other measurement techniques. They used hot-wire anemometry (HWA) to experimentally investigate jet flows. It provides single point spectral analysis of the turbulent flow, due to high sampling rates. (Wernet, 2007 et al)PIV is widely used to measure the large regions of unsteady flow field in sequential frames, but it has a lower frequency than the other measurement techniques such as HWA. The above

described studies were experimental and gave an insight about the experimental techniques.

Bogey et al. predicted the turbulent flow characteristics and acoustic fields of a subsonic circular jet with a Mach number of 0.9 and moderate Reynolds number using LES. Noise radiated by the jet predicted by computational techniques was in good agreement with experimentally measured data from the literatures. They investigated the effects of intrusion of vertical structure into the jet core. RANS and LES are the widely used computational models for the prediction of turbulent and noise characteristics of the jets. Tucker et al., used three different FW–H surfaces to calculate the acoustic quantities turbulent jets. Numerical predictions were compared with the experiments and the results were generally good, but at the higher frequencies computational results showed larger deviation from the experiments, it interpreted that it's an indication to use finer grids for the simulation. Engblom et al. [15] presented numerically predicted the flow performance and far-field acoustics of a single stream chevron nozzle. To predict the far-field noise distributions the outputs from the WIND flow solver (Steady Reynolds Averaged Navier Stokes) solution from the WIND flow solver was provided as an input to the MGBK acoustics code. Direct comparison with experimental data was made. The parameters such as PIV turbulent kinetic energy fields, stagnation pressure and temperature rake data and 90 degree observer far-field microphone data were compared with the numerical results. Although there were some inaccuracies observed, they presented that the effects of chevron were promising in improving the mixing.

The objective of the present study is to study utilizing the ability of RANS calculations with an SST turbulence model to simulate flow field characteristics of round, subsonic jets with and without chevron at the exit. Although LES may give much better results than the RANS approach, it is preferred for its less computational requirements and also, it has been used as an efficient design tool, for comparative studies of different nozzle designs. All the calculations have been done using ANSYS CFX.

MODEL DESCRIPTION AND METHODOLOGY

All nozzles have same exit area but, their exit was fitted with different chevron configuration. Three different chevron configurations according to the number of chevrons have been considered for current study, which are no chevron (plain jet), 4 chevrons and 8 chevrons. For all the nozzle configurations inlet area ($4430 mm^2$) and exit area ($506.7 mm^2$) were maintained constant irrespective of the chevron configuration. The chevrons were attached at the exit of the nozzle the axial length of the chevron is 5mm. All the chevrons have zero penetration angle to the jet axis. Chevrons were slightly blunted at the edge. Chevron arrangements with nozzle were presented in figure 1.

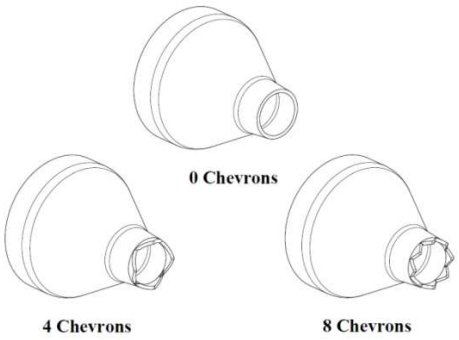

Figure 1: Different Nozzle Exit Geometry Considered for Present Study

Meshing

The fluid flow domain is discredited into a 3D grid consist of unstructured tetrahedral elements which has four faces and four nodes. The region which surrounds the jet flow is constructed with fine grid elements to accurately capture the boundary layer and jet decay properties. Total number of nodes and elements approximately used for present study were 300000 and 1600000 respectively.

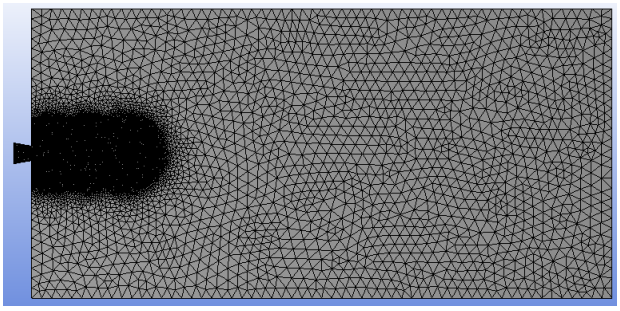

Figure 2: Mesh Distribution

Physics Definition

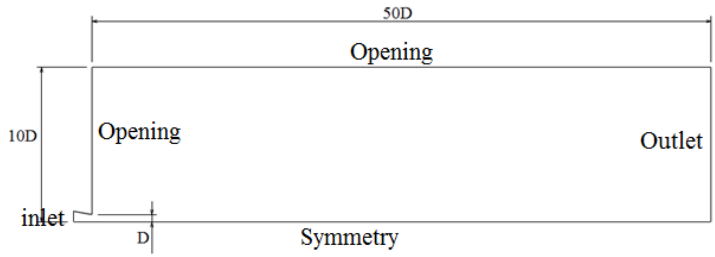

Figure 3: Domain Based on Jet Dia (D = 12.7mm) Pedro Ricardo C

The updated mesh files were loaded into the CFX-Preprocessor (CFX-Pre). The steady state RANS computational model is used to simulate the considered flow field. For present study, inlet boundary is specified with total pressure that had been calculated using isentropic relation for the compressible flows using Mach number at the exit plane. Ambient pressure and temperature at sea level were specified (P_∞=101325Pa, T_∞=288K) at the opening boundary. The outlet has been specified with the static pressure. Two equation Shear Stress Turbulence model (SST) was used for predicting turbulence accurately which offers optimal switching between k-ϵ and k-ω turbulence model at appropriate node points. The SST model shifts values between one and zero of F_{sst} (the blending function) from near wall to open regions. The switching formulation is a combination of instructions based on proper blending functions of k-ϵ and k-ω regions without user interaction. It gives a smooth switching between k-ϵ and k-ω turbulence model with high resolution (Gopinath et al).

RESULTS AND DISCUSSIONS

In this study centerline velocity decay along the jet axis and turbulent kinetic energy were presented. Effects of exit Mach number and number of chevrons on the above properties were analyzed in detail.

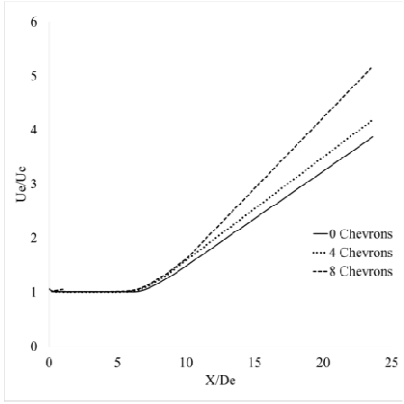

Figure 4: Centerline Velocity Decay of Mach 0.4 Jet

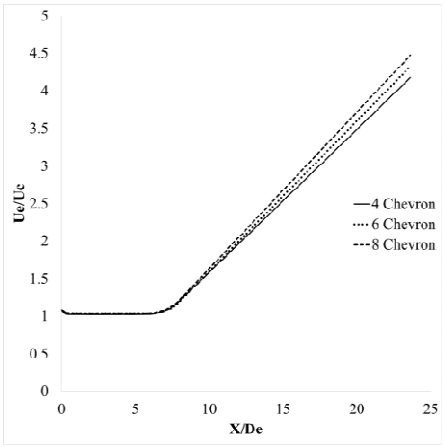

Figure 5: Centerline Velocity Decay of Mach 0.6 Jet

Figure 4 shows the centerline velocity decay of the 0.4 Mach jet. Three exit conditions were compared which are no chevron (0 chevron), 4 chevron abd 8 chevron nozzles. All the three configurations has the exit Mach number of 0.4. The X axis of the plot represents centerline location and its non-dimensionalized, using the exit diameter De of the nozzle which is equal to 0.0254mm. Y axis of the plot represents the centerline velocity which is non-dimensionalized using the exit velocity. From observing the plot solid lines represent the 0 chevron configuration, dotted line represents the 4 chevron configuration and dashed line represent the 8 chevron configuration. In the plot there is a constant velocity region is observed from X/De = 0 to X/De = 6 and its known as potential core length. Region between X/De = 6 to X/De = 12 is known as transition decay region. The region X/De >12 is known as self-similar region. Potential core length of 0 chevron region ends at X/De = 6. It can be observed from the plot the potential core length is comparatively shorter for the 4 and 8 chevron configurations which extends up to X/De = 5.2. It is one of the important parameters that indicates the jet has improved mixing. But, there is no significant difference is observed between the potential core length of 4 and 8 chevron configurations. By observing the self-similar region the slope of the 0 chevron is comparatively smaller than the self-similar region of 4 and 8 chevron jets. Among the three configurations considered, the 8 chevron configuration has the maximum decay rate at the self-similar region. This results in improved mixing. Figure 5 shows the centerline velocity decay of Mach 0.6 jets with different exit conditions. By observing the plot lines it can be seen that the potential core length for all the three configurations are similar and equal to X/De = 6. Although the jets have the same potential core length there is considerable difference in the velocity decay rate were observed. Among the three configurations considered 8 chevron has the highest decay rate and 0 chevron has the lowest decay rate. From the above two configurations it can be

said that the length of the potential core is less sensitive to the chevron when the exit Mach number of that is increased from 0.4 to 0.6. Although the decay rate increases with number of chevrons it is observed that the difference in decay rate grows lower between the configurations.

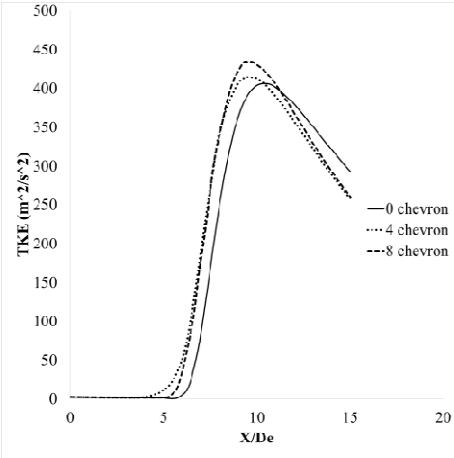

Figure 6: Centerline Turbulent Kinetic Energy of Mach 0.4 Jet

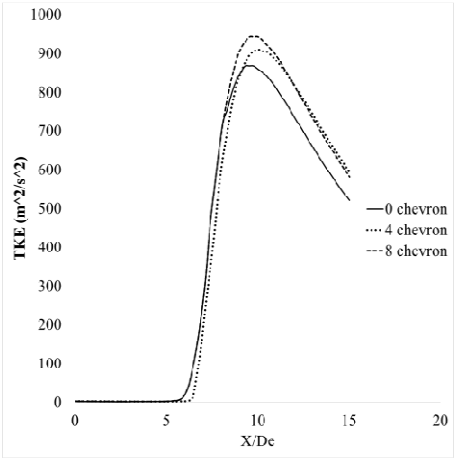

Figure 7: Centerline Turbulent Kinetic Energy of Mach 0.6 Jet

Figure 6 shows the centerline turbulent kinetic energy (TKE) with respect to its centerline location. X axis represents the centerline location and non-dimensionalized using the diameter of the nozzle exit (De). A considerable difference is observed between the TKE of the different chevron configuration. For the no chevron configuration case the TKE stands to increase sharply after X/De = 6. But the TKE for the 4 chevron configuration starts to increase from X/De = 4 itself. The TKE for the 8 chevron starts to increase at X/De = 5. Although the TKE starts to increase at X/De = 5 and reaches its maximum value around X/De = 10. 0 chevron has the lowest TKE peak value than the other two configurations and 8 chevron has the highest TKE peak value. This may be the reason for the 8 chevron jet has the maximum decay rate when compared with other two configurations.

Figure 7 shows the centerline TKE distribution for Mach 0.6 jet. From the plot it can be observed that the 0 and 8 chevron has similar profile. But the peak TKE value significantly defers from the 8 chevron jet and it's the maximum of all configuration. Plain jet has lowest amount TKE peak value at the centerline as observed in the previous case. From the TKE plots it can be said that the maximum TKE peak jet has higher decay rate and the minimum decay rate and the minimum TKE peak value jet has lowest decay rate.

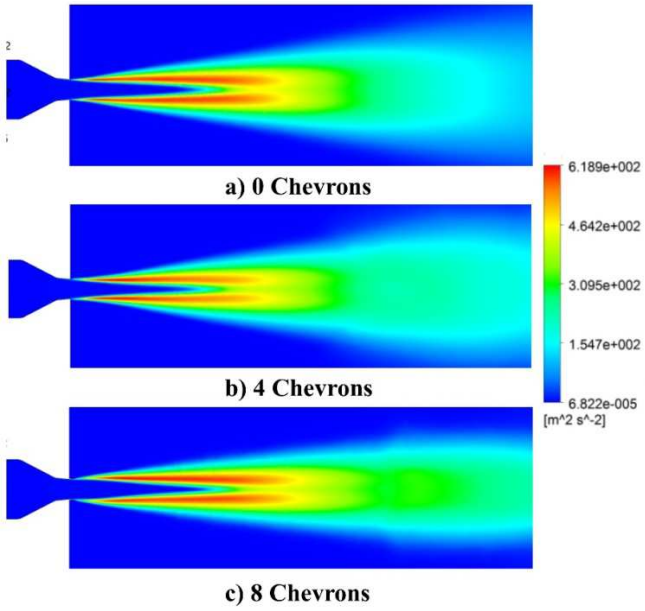

Figure 8: Turbulent Kinetic Energy Distribution of 0.4 Mach Jets

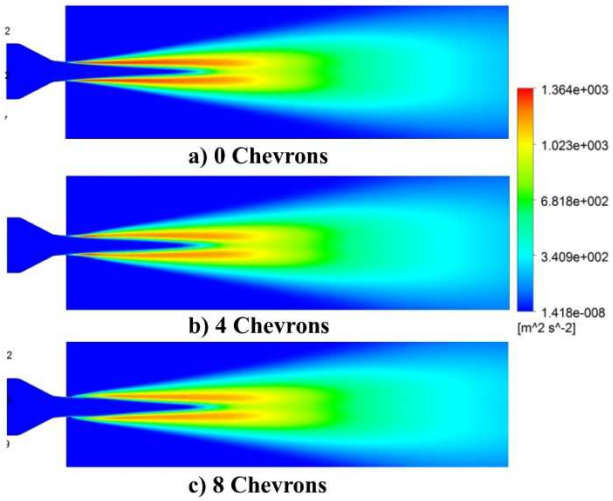

Figure 9: Turbulent Kinetic Energy Distribution of 0.6 Mach Jets

Figure 8& 9 shows the TKE distribution at the symmetric plane for 0, 4 and 8 chevron configurations with the exit Mach number of 0.4 and 0.6 respectively. It can be seen that the 0 chevron jet has not much dispersion of TKE when compared with other 2 configurations. The red colored region shows the strong shear layer location where the maximum difference in interface velocity occurs. The shear layer starts from the nozzle exit and propagates towards downstream. Its thickness also significantly increases with the distance from the exit. This shear layer region is significantly important for the mass from the surrounding environment to enter into the jet flow. This elevate the mixing process and results in better jet decay profile.

CONCLUSIONS

In the present study, the flow fields generated by circular jets with a chevron and a conventional circular nozzle exits are studied and compared. Three different nozzle configurations were considered one with no chevron and the other

two has 4 and 8 chevrons each. Each configuration, has studied with two different exit Mach numbers. It can be said that the length of the potential core is less sensitive to the chevron when the exit Mach number of the jet is increased from 0.4 to 0.6. Although the velocity decay rate increases with number of chevrons, it is observed that the difference in decay rate grows smaller between the configurations when the Mach number is increased. For both exit Mach number conditions maximum value of TKE peak occurs for the 8 chevron configuration and thus the decay rate.

REFERENCES

1. *Davies, P.O.A.L., Fisher, K.J., and Barratt, M.J. (1963). The characteristics of turbulence in the mixing region of a round jet, J Fluid Mech 15, 337-367.*
2. *Bradshaw, P., Ferriss, D.H., Johnson, R.F. (1963). Turbulence in the noise-producing region of a circular jet, J Fluid Mech 19, 591-625.*
3. *Bridges, J. and Wernet, M. P. (2010). Establishing Consensus Turbulence Statistics for Hot Subsonic Jets," AIAA Paper 2010-3751, 16th AIAA/CEAS Aeroacoustics Conference, Stockholm, Sweden.*
4. *Wernet, M. P. (2007). Temporally resolved PIV for space-time correlations in both cold and hot jet flows, Measurement Science and Technology, vol. 18, pp. 1387–1403.*
5. *Bogey C, Bailly C, Juve D. (2003). Noise investigation of a high subsonic, moderate Reynolds number jet using a compressible large eddy simulation. TheorComput Fluid Dyn 16, 273–97.*
6. *Jeong-Sik Park et al., Noise Reduction Based on Robust Speech and Non-Speech Detection in Vehicular Environments, International Journal of Mechanical and Production Engineering Research and Development (IJMPERD), Volume 7, Issue 3, May - Jun 2017, pp. 105-112*
7. *Tucker PG. Miles N. (2004) computations for jet flows and noise. Int J Heat Fluid Flow 25:625–35.*
8. *Engblom WA, Khavaran A, (2004). Bridges J. Numerical prediction of chevron nozzle noise reduction using WIND-MGBK methodology. AIAA-2004-2979.*
9. *Pedro Ricardo C. Souza and Odenir d Almeida (2012). "Aerodynamics Characterization of A Subsonic Jet: Boundary Conditions Influence", Thesis, Federal University of Uberlândia, Brazil.*
10. *Gopinath, S, Sundararaj, M., Elangovan, S., et al. (2014). Mixing Characteristics of Elliptical and Rectangular Subsonic Jets with Swirling Co-flow. International Journal of Turbo & Jet-Engines, 32(1), pp. 73-83.*
11. *Hope Nzewi & Dadzie Bawo Cynthia, Outsourcing Strategy and the Performance of Chevron Nigeria Limited, International Journal of Business Management & Research (IJBMR), Volume 5, Issue 2, Mar - Apr 2015, pp. 95-106*
12. *Vijayaraja, K, Senthilkumar, C., Elangovan, S., et al. (2013). Base Pressure Control with Annular Ribs. International Journal of Turbo & Jet-Engines, 31(2), pp. 111-118. Retrieved 21 Aug. 2017*